A Cell-Semiconductor Synapse: Transistor Recording of Vesicle Release in Chromaffin Cells

Janosch Lichtenberger and Peter Fromherz
Department of Membrane and Neurophysics, Max Planck Institute for Biochemistry, Martinsried/Munich, D 82152 Germany

ABSTRACT The release of dense-core vesicles in bovine chromaffin cells is a model for the presynaptic process in neurons. It is usually studied by microamperometry of catecholamines with carbon fibers. Here we introduce transistor recording as a tool to study vesicle release. When we stimulate a chromaffin cell placed on a field-effect transistor, the gate voltage exhibits peaks that correlate with a simultaneously performed amperometric recording. We attribute the transistor signal to a release of protons from the extruded matrix of vesicles that lowers the extracellular pH and changes the electrical surface potential of the gate oxide. The rise time of the transistor signals is similar to that of amperometric responses, whereas their duration is distinctly longer. In a model computation, the rise time is identified with the extrusion of vesicle matrix into the narrow extracellular space between cell and gate oxide, and the decay time is attributed to pH equilibration through slow diffusion in the extruded matrix. Because the transistor recording relies on protons, it can be applied to acidic vesicles with electrochemically inactive hormones or transmitters.

INTRODUCTION

Vesicle exocytosis is an important process in neuronal signaling. It controls the release of transmitters in the presynaptic neuron and elicits a specific response of receptors in the postsynaptic cell. A detailed experimental investigation of the release dynamics became possible when carbon fibers were introduced as fast and sensitive amperometric detectors (1–3). The hormonal exocytosis of chromaffin cells became a particularly important model system because of the large size of their dense core vesicles and the electrochemical reactivity of the released catecholamines. Crucial aspects of exocytosis were elucidated in combination with capacitance measurements and fluorescence techniques (4,5). In an early step of the release process, soluble components permeate through a pore formed by the membranes of the vesicle and the cell. In a subsequent step, the vesicle membrane unfolds, and the chromogranin matrix of the vesicle is extruded (6,7).

Field-effect transistors with an open gate oxide in an electrolyte have been used to record the electrical activity of individual nerve cells (8). In this study, we introduce transistors as probes for the exocytosis of vesicles. The concept is sketched in Fig. 1 *A*. A chromaffin cell is attached to the gate oxide of a field-effect transistor. When a vesicle fuses with the plasma membrane, its content is released into the narrow extracellular space between cell and chip. Because of the low pH 5.5 and the high buffer capacitance of a vesicle (9,10), we expect a local drop of the extracellular pH. As a consequence, the protonation of the gate oxide is enhanced. The concomitant change of the electrical surface potential leads to a modulation of the source-drain current as in a classical ion-sensitive field-effect transistor (11).

Four aspects may render the transistor recording of vesicle release useful in addition to amperometry: 1), The proton mechanism of recording may enable a study of acidic vesicles (12) with electrochemically inactive hormones and transmitters. 2), The mechanism of detection may provide additional information on vesicle release. 3), Large arrays of transistors allow a parallel recording of many cells for biosensor applications. 4), Transistor arrays may be able to record synaptic activity and electrical excitation in a neuronal network simultaneously.

MATERIALS AND METHODS

Transistors

We use silicon chips with a linear array of 96 p-channel field-effect transistors (13). The metal-free gates made of silicon dioxide have an area of 2 μm $\times$ 20 μm. A perspex chamber is attached to the chip with a shape that provides laminar flow of the bath solution. The chips are cleaned with a dishwashing detergent and rinsed with 80°C deionized water. They are UV sterilized and coated with collagen (C9791, Sigma-Aldrich, St. Louis, MO) by adsorption from a 50 μg/ml solution in deionized water for 2 h at 37°C.

The operating point of the transistors is adjusted by a bias voltage of 0.5 *V* between source and drain and of 0.7 *V* between bulk silicon/source and the bath contacted with an Ag/AgCl electrode (World Precision Instruments, Sarasota, FL) that is held on ground potential. The transient signals of the transistor to the activation of chromaffin cells are high-pass filtered at 0.16 Hz to reduce the drift, low-pass filtered at 1 kHz, and sampled at 2 kS/s.

We calibrate the changes of the source-drain current in terms of changes of the gate voltage immediately before each measurement by applying voltage steps to the bath electrode. The transconductances are ~ -130 nA/mV. A calibration in terms of pH changes on the gate is difficult to perform for each measurement without damaging the cell-chip system. We estimate the relation of the voltage change and the pH change by pH titration of transistors with a salt bridge for the reference electrode. For fresh chips we find a slope in a range of -20 to -30 mV/pH. After cell culture, the slope is lowered to ~ -10 mV/pH. The oxide seems to be ''passivated'' by cell culture, cleaning, and coating with a lower density of dissociable silanol groups. When we change the normal electrolyte with high NaCl concentration to a high KCl concentration, a signal of $\sim +20$ mV is induced as a

Submitted September 1, 2006, and accepted for publication December 7, 2006.

Address reprint requests to Peter Fromherz, E-mail: fromherz@biochem.mpg.de.

0006-3495/07/03/2262/07 $2.00

doi: 10.1529/biophysj.106.096446

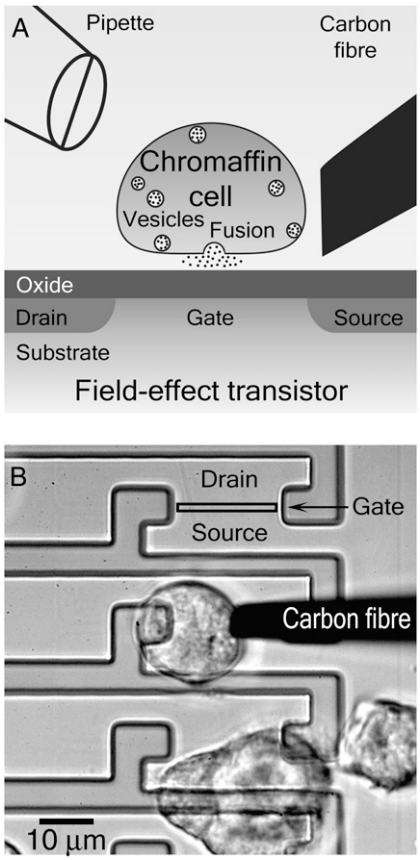

FIGURE 1 Chromaffin cell on a transistor. *(A)* Schematic cross section (not to scale, cell diameter ~15 μm, cell-chip distance ~50 nm). Vesicles are released into the narrow extracellular space between cell and transistor. A carbon fiber is used for amperometry. Exocytosis is elicited by $BaCl_2$ applied with a pipette (θ-tube). *(B)* Micrograph of silicon chip with linear transistor array. Source, drain, and gate (*black frame*) are marked on the upper transistor. A chromaffin cell covers about one-half of the open gate area (2 μm × 20 μm). The cell is touched by a carbon fiber from the right.

result of K^+ binding to the oxide (14). A change of pH sensitivity is not observed. Binding of epinephrine and ATP is negligible as checked by titration.

Chromaffin cells

Bovine adrenal glands are obtained from the local abattoir. Chromaffin cells are prepared by enzymatic digestion (15). They are cultured on the coated silicon chips in enriched DMEM (Linaris, Wertheim-Bettingen, Germany) containing 2 g/liter $NaHCO_3$, 4.5 g/liter D-glucose, 1.028 g/liter L-glutamine, 10 ml/liter insulin-transferrin-selenium-X (Invitrogen, Carlsbad, CA), and 1:250 penicillin and streptomycin (10,000 U/ml; Linaris). Two hours after seeding, 5% fetal bovine serum (Invitrogen) is added to the medium. Experiments are performed after 1 to 3 days.

Solutions

Vesicle release is induced by 3 mM $BaCl_2$ using a θ-tube (Hilgenberg, Malsfeld, Germany) pulled to an inner diameter of 180 μm and mounted on a piezo actuator (16). The solutions are delivered by a syringe pump at a rate of 2 ml/h. To avoid pollution with Ba^{2+} ions, the chamber is continuously perfused with a bath solution at 2 ml/min. We use three different solutions with an osmolarity of 320 mOsm at a pH 7.2: 1), 5 mM HEPES with 140 mM NaCl, 2.8 mM KCl, 2 mM $MgCl_2$, and 35 mM glucose; 2), 10 mM HEPES with 137.5 mM NaCl, 2.8 mM KCl, 2 mM $MgCl_2$, and 30 mM glucose; or 3), 20 mM HEPES with 132.5 mM NaCl, 2.8 mM KCl, 2 mM $MgCl_2$, and 15 mM glucose. For the histograms of buffer action on the transistor signals, 484 peaks of 9 cells are evaluated at 5 mM HEPES, 450 peaks of 9 cells at 10 mM, and 342 peaks of 10 cells at 20 mM. For experiments with equilibrated pH across the vesicle membrane, nigericin and valinomycin (Fluka & Riedel, Seelze, Germany) in ethanol are added at concentrations of 3 μM and 5 μM, respectively, to a solution with 80 mM KCl in combination with lowered NaCl concentration.

FLIC measurements

The distance between silicon dioxide and the plasma membrane of chromaffin cells is determined by fluorescence interference contrast (FLIC) microscopy (17). The FLIC chips are cleaned and coated by the same procedure as the transistor chips. The cells were stained with the cyanine dye $DiC_{18}(3)$ (Molecular Probes, Eugene, OR). The fluorescence intensities on four oxide terraces are determined and fitted by the FLIC theory.

Amperometry

Before a measurement a carbon fiber of 5 μm diameter (ALA Scientific Instruments, Westbury, NY) is cut and dipped into isopropanol for a few seconds. It is gently pressed against the cell membrane to achieve local detection of vesicle release and held at 800 mV versus Ag/AgCl. The current is recorded with a bandwidth of 1 kHz. For the histograms of buffer action, the carbon fiber was placed on the upper cell membrane, and 354 peaks of five cells were evaluated at 5 mM HEPES, 457 peaks of five cells at 10 mM, and 493 peaks of seven cells at 20 mM.

Numerical simulation

In a theoretical model we compute the release of a vesicle into the cleft between the chromaffin cell and the transistor. We assume that the vesicle matrix is extruded at a constant volume flux so that a pancake is formed on the gate oxide with a constant rate. In contact with the extracellular solution, the solutes of the vesicle with 110 mM ATP, 500 mM epinephrine, 20 mM NaCl at pH 5.5 diffuse into the surrounding cleft and the solutes of the cleft diffuse into the matrix. All diffusion coefficients in the matrix are assumed to be reduced by a factor 1/100 with respect to the values in the electrolyte of (in μm^2/ms) H^+ 9.31, Na^+ 1.33, Cl^- 2.03, HEPES 0.79, ATP 0.4, and epinephrine 0.6. The reaction of protons with ATP, HEPES, and the silanol groups of the oxide is assumed to be fast (18) with pK values of 7.52 for HEPES and 6.5 for ATP and with an intrinsic $pK_i^{sil} = 5.9$ for the silanol groups of the oxide (19).

We compute the diffusion of all species along the narrow extracellular cleft of the cell-chip junction with an Euler forward algorithm. Gradients of the electrical potential along the cleft are neglected because of the high salt concentration. The simulation is performed on two quadratic grids, one for the area of release (mesh width 0.02 μm on 1 μm × 1 μm), and another for the rest of the cell-chip junction (mesh width 0.2 μm on 16 μm × 16 μm). The concentrations across the cell-chip junction are assumed to be equilibrated because the diffusion across the narrow cleft as well as the buffer reactions are fast compared to lateral diffusion. Within each iteration step, we compute the electrical double layer of the oxide/electrolyte interface with the one-dimensional nonlinear Poisson-Boltzmann equation by a Newton-Raphson algorithm (20) taking into account all ions in the electrolyte and all buffer equilibria. The density of surface charges is given by the dissociated silanol groups.

RESULTS

Transistor recording and amperometry

A chromaffin cell on the open gate of a transistor is shown in Fig. 1 *B*. The cell has a diameter of 15 μm and covers one-half of the gate with an area of 2 μm $\times$ 20 μm. The distance between the cell membrane and the oxide surface is ~50 nm measured by FLIC microscopy. A carbon fiber is gently pressed to the cell membrane and to the transistor surface. Using a θ-tube, we apply a 10-s pulse of 3 mM $BaCl_2$ that induces a release of vesicles for several minutes (21). The responses of the transistor and of the carbon fiber are shown in Fig. 2 *A*. In both traces we see a stochastic sequence of sharp events. Within 5 min there are 282 peaks in the transistor signal with amplitudes up to 5 mV, whereas the amperometric record exhibits 243 current pulses.

The overall distribution of the events in time is similar for the transistor recording and for the carbon fiber. We find 111 pairs of events with a distinct correlation in time so that the amperometric response is recorded within 10 ms after a transistor signal. The 79 events that appear within a time window of 5 ms are indicated by the bars in the center of Fig. 2 *A*. The amplitudes of amperometric records that are correlated with transistor signals are usually lower than uncorrelated signals, and their width is broader.

An example of two coincident signals is plotted in Fig. 2 *B*. The amperometric current rises within 2 ms and decays within 10 ms. Before the main signal there is a ''foot structure'' with a duration of ~40 ms that is known to indicate a first stage of vesicle fusion (7). The main transistor signal also rises within 2 ms. However, it decays distinctly more slowly over 40 ms. There is a weak response before the main signal, in analogy to the foot structure of amperometry.

Considering the frequency of events as well as the shape of the individual signals, we conclude that the events of the transistor record are caused by the release of individual dense-core vesicles in analogy to the events of amperometry. We assign correlated events with delayed amperometric spikes to fusion sites near the periphery of cell adhesion so that released substances can reach the carbon fiber by diffusion along the cleft. The different waveform of the two kinds of signals must be attributed to the different mechanisms of the two recordings.

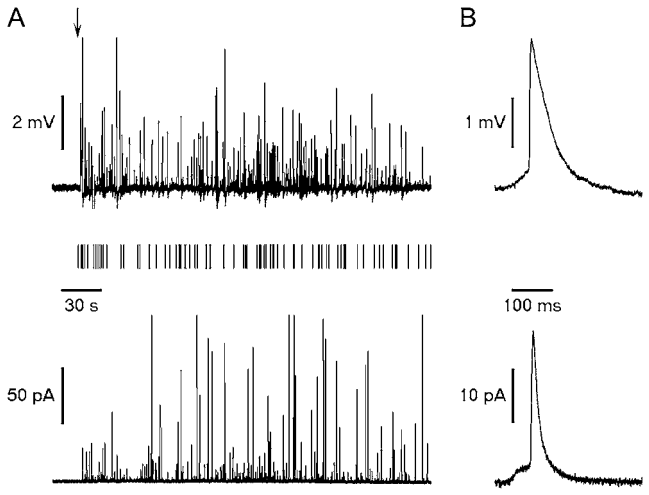

FIGURE 2 Simultaneous detection of vesicle release by transistor recording and amperometry. *(A)* Distribution of events in time for the transistor signal *(top)* and amperometry *(bottom)*. The stimulation by a pulse of 5 mM $BaCl_2$ is marked by an arrow. The band of vertical bars between the two records marks the events that are detected by the transistor and the carbon fiber within a time window of 5 ms. *(B)* Transistor record *(top)* and amperometry *(bottom)* of a coincident event with a foot structure and a main signal.

Proton signal

In principle, the signal of a field-effect transistor beneath an attached cell may indicate a changed voltage drop in the electrical double layer from the oxide surface to the cell-chip junction or a voltage in the cell-chip junction with respect to the bath electrolyte (14). However, during the vesicle release of a chromaffin cell, there is no flow of electrical current that would give rise to a voltage in the cell-chip junction as is observed with open ion channels (13,14). Thus, the transistor signal must be caused by an effect on the electrical double layer.

We assign the observed voltage signal to a change of the pH in the cell-chip junction that is caused by the acidic content of dense-core vesicles. The transistor plays the role of a classical ion-sensitive field-effect transistor. Two experiments are performed to verify this hypothesis: 1), we abolish the low pH in the vesicles, and 2), we enhance the concentration of extracellular acid-base buffer.

The low pH in dense-core vesicles breaks down when nigericin and valinomycin are added to promote an equilibration of protons across the vesicle membrane (22). Using the θ-tube, we apply $BaCl_2$ in an electrolyte with nigericin/valinomycin and an enhanced KCl concentration. The signals of transistor recording and of amperometry are shown in Fig. 3. At first there is a burst of events followed by a period of 30 s with low activity. After this initial phase, a series of events is observed by the carbon fiber as well by the transistor. However, the amplitudes of the transistor record are very weak, whereas the amplitudes of the amperometric signal are quite normal. Thus, the events of the transistor recording are related to the intravesicular pH.

In a second approach, we enhance the concentration of extracellular HEPES buffer from 5 mM to 20 mM and observe the events of the transistor recording and of the amperometry before and after the change. Fig. 4 *A* shows the average of the five highest peaks in an experiment. Apparently, the amplitude and the duration of transistor signals are lowered, whereas the amperometric signals remain unchanged. The integral distribution of rise time, decay time, and amplitude of the transistor records and of the amperometric signals

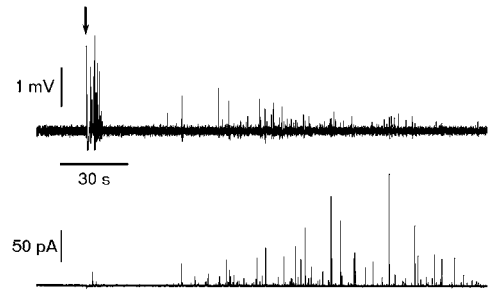

FIGURE 3 Effect of equilibrated pH across the vesicle membrane. $BaCl_2$ is added together with nigericin and valinomycin at a raised potassium concentration (*arrow*). After an initial burst and a phase of suppressed release, the amplitudes of the events in the transistor signal *(top)* are low, whereas the events of the amperometric current *(bottom)* have normal amplitudes.

from numerous experiments are shown in Fig. 4 *B* with 5 mM, 10 mM, and 20 mM HEPES. The wide variation of the signals is caused by the distribution of vesicle size (23). For the transistor records, the median of the rise time is invariant around 2 ms, the median of the half-width drops from 35 ms to 16 ms and to 11 ms, whereas the median of the amplitude drops from 1.4 mV to 0.9 mV and to 0.6 mV. With amperometry the buffer concentration has no effect with constant medians of the rise time (2.5 ms), of the half-width (11 ms), and of the amplitude (20 pA).

We conclude that the events of transistor recording during vesicle release are caused by a proton signal, similar to recordings by pH-sensitive fluorescent dyes (24). Amplitude and half-width of the signals are determined by the dynamics of pH in the extracellular space.

DISCUSSION

Field-effect transistors are able to detect the release of individual dense-core vesicles from chromaffin cells. The discrete signals are caused by a release of protons that gives rise to a low pH in the narrow extracellular space between the cells and the oxide surface of the chip. The local pH change is detected by the transistor with a response time that is similar to that of amperometry.

To explain details of the transistor signals, we consider two approaches: At first, we discuss how the dynamics of the extracellular pH are affected by acid-base buffers in the cell-transistor junction. Then we describe a model that relies on an extrusion of the vesicles and a slow diffusion within the released matrix.

Buffer model

We assume that the release of protons is coupled to the fast release of catecholamine indicated by the amperometric signal. The question is whether the slow decay of the transistor records results from an effect of acid-base buffers.

We take into account a mobile HEPES buffer with a concentration c_J^{HEPES} in the cell-chip junction and an immobile buffer of silanol groups on the oxide with an effective concentration $c_J^{sil} = \sigma^{sil}/d_J$, where σ^{sil} is the density of silanol groups, and d_J is the width of extracellular space. For fast equilibration with the dissociation constants K^{HEPES} and K^{sil} and without buffer saturation, the effective diffusion coefficient D_J^H of protons is given by Eq. 1 with the diffusion coefficient D_J^{HEPES} of the mobile buffer (25).

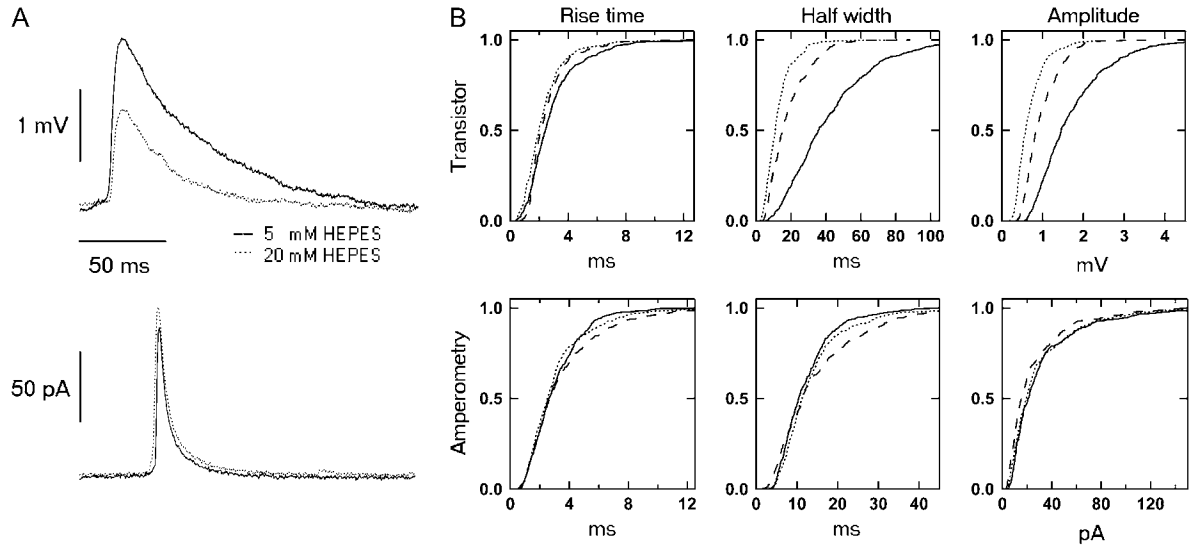

FIGURE 4 Effect of acid-base buffer on transistor recording and amperometry. *(A)* Average of the five highest signals in an experiment, where 5 mM HEPES is replaced by 20 mM HEPES. *(B)* Integral distribution functions of rise time, duration, and amplitude of transistor recording *(top)* and of amperometry *(bottom)* for 5 mM HEPES (*drawn*), 10 mM (*dashed*), and 20 mM (*dotted*). An enhanced concentration of acid-base buffer affects the time course and the amplitude of the transistor events, but not of amperometry.

$$\frac{D_J^H}{D_J^{HEPES}} = \frac{1}{1 + \left(c_J^{sil}/c_J^{HEPES}\right)\left(K^{HEPES}/K^{sil}\right)} \quad (1)$$

For $d_J = 50\,nm$ and an upper limit $\sigma^{sil} = 5\times10^{14}cm^{-2}$ (19), the concentration of the immobile buffer is $c_J^{sil} = 170\,mM$. Considering $K^{sil} = K_i^{sil}\exp(\varphi_S/25\,mV)$ with an intrinsic dissociation constant $K_i^{sil} = 2\,\mu M$ and a negative surface potential in the order of $\varphi_S \approx -100\,mV$ we obtain with $c_J^{HEPES} = 5....20\,mM$ and $K^{HEPES} = 63\,nM$ the relation $(c_J^{sil}/c_J^{HEPES})(K^{HEPES}/K^{sil}) \gg 1$. Based on Eq. 1 we would expect 1), that the diffusion of protons and the relaxation of pH are slowed down by the immobile buffer, and 2), that it is accelerated by an enhanced concentration of HEPES. Both conclusions are in agreement with the experiment. However, the model cannot describe the reduction of the signal amplitude by enhanced HEPES concentrations because the total buffer capacitance is determined by the high concentration of the immobile buffer. A change of the amplitude by HEPES would be achieved only if its concentration dominates with $c_J^{HEPES} \gg c_J^{sil}$. In this case the proton diffusion would be fast and little affected by HEPES according to Eq. 1, in contradiction to the experiment. A local saturation of the mobile and immobile buffers would lower the effects on amplitude as well as on duration. Acid-base buffers alone are not able to explain the dynamics of the transistor signals.

Extrusion model

Strong stimulation of chromaffin cells leads to an extrusion of the complete vesicle content including the chromogranin matrix (6). The involved process implies an expansion of the fusion pore, a concomitant enhancement of the release area, expulsion of the matrix, a swelling of the matrix by osmotic effects and ion exchange, slow diffusion of small molecules within the matrix, and a diffusion to the extracellular medium. We consider a simplified model to explain the response of a transistor with an attached chromaffin cell. First, we assume that the vesicle matrix is squeezed into the narrow cleft between cell and chip. Second, we consider slow diffusion in the pancake of extruded matrix and normal diffusion in the surrounding extracellular space. The resulting change of pH on the gate, in the area of the extruded matrix and beyond, determines the average change of the voltage drop in the electrical double layer of the gate oxide.

In a computer simulation (see Methods), we assume that the matrix of a vesicle with a typical diameter of 340 nm (23) expands at a constant rate to form a pancake with a diameter of 0.75 μm on the gate and a thickness of 50 nm. The diffusion coefficients of protons, ATP, epinephrine, HEPES, and NaCl are assumed to be lowered in the matrix compared to the extracellular space. All buffers are assumed to be locally equilibrated. For the silanol groups of the oxide, we assume a single intrinsic dissociation constant with $pK_i^{sil} = 5.9$. The dissociated silanol groups determine the surface potential as described by the Poisson-Boltzmann equation. We match the transistor record with 5 mM HEPES by choosing an extrusion time of 3 ms, a reduction of all diffusion coefficients in the matrix by a factor 1/100 as was considered for epinephrine and serotonin (6,26), and a low density of $0.5\times10^{14}cm^{-2}$ for the silanol groups. The values of all other parameters are given in the Methods section.

Fig. 5 *A* shows the pH profiles at 3, 7, and 20 ms after the start of extrusion for 5 mM HEPES. In the initial phase, a change of $\Delta pH = -1.6$ arises in the area of the extruded matrix. Later, that local effect decays, and a change of pH appears in the surround. In Fig. 5 *B* the concomitant changes of the surface potential are plotted with an initial local change of $\Delta\varphi_S = 40\,mV$. Part of that change results from proton binding to the silanol groups, with a minor component

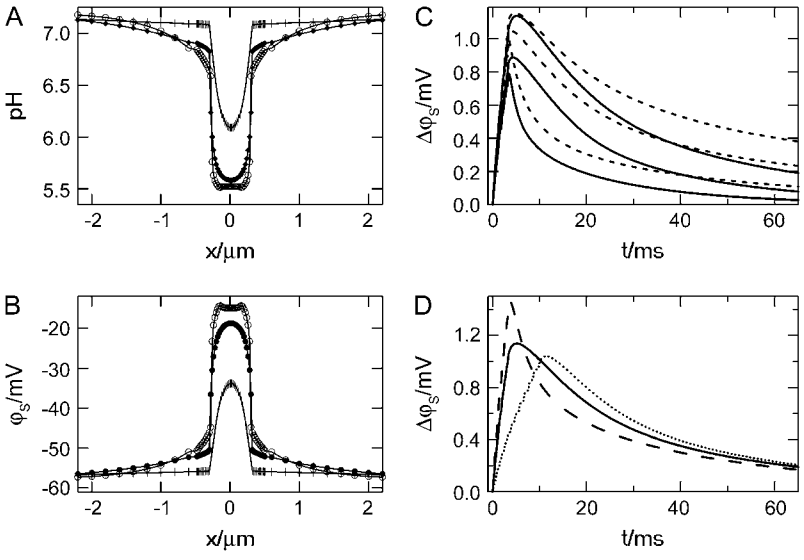

FIGURE 5 Extrusion model of transistor recording. *(A)* Profiles of pH along cell-transistor junction at 3 (*open circles*), 7 (*solid circles*), and 20 ms (*bars*) after the start of matrix extrusion for 5 mM HEPES. The parameters (optimal) are 3 ms extrusion time, a factor 1/100 for the reduction of diffusion coefficients, and a density of $0.5\times10^{14}cm^{-2}$ of silanol groups. *(B)* Profiles of the electrical surface potential φ_S along the gate oxide. At 3 ms, the changes of pH and surface potential are well localized in the area of the extruded matrix. Later, the local responses decay, and transient signals appear in the surrounding. *(C)* Average change of surface potential $\Delta\varphi_S$ versus time for 5, 10, and 20 mM HEPES (*from top to bottom*) with optimal parameters (*drawn line*) and with a high density $5\times10^{14}cm^{-2}$ of silanol groups (*dashed line*). *(D)* Average surface potential for 5 mM HEPES with optimal parameters (*drawn line*), with 10 ms extrusion time (*dotted line*), and with a factor 1/10 for the reduction of diffusion coefficients (*dashed line*). The extrusion model with optimal parameters accounts for amplitude and shape of the transistor records and for lowered amplitude and duration with enhanced buffer concentration.

caused by the high salt concentration in the matrix. From the profile of the surface potential on the whole gate area of 2 μm $\times$ 20 μm, we compute the average change of the surface potential. The result is shown in Fig. 5 *C* (*drawn lines*). There are a fast rise up to 1.2 mV within 3 ms – determined by the large local change in the area of the matrix and a slow decay within 35 ms that is related to the changes on the whole gate. The decay of the signals is quite slow despite the low concentration of the immobile buffer. When the concentration of HEPES is enhanced from 5 mM to 10 mM and 20 mM, both the amplitude and the duration of the signals are lowered in the model, as shown in Fig. 5 *C*, an effect that is in agreement with the experiment but not described by the simple buffer model.

We check the validity of the extrusion model by variation of the three crucial parameters: the extrusion rate, the density of silanol groups, and the diffusion coefficients in the matrix. 1), A computed signal with an extrusion time of 10 ms is shown in Fig. 5 *D*. The slow increase of the signal does not match the observed signal. Within the model we can attribute the rise time of the transistor record to the rate of the matrix extrusion. 2), The effect of a high density of silanol groups of 5×10^{14}cm^{-2} is shown in Fig. 5 *C*. The amplitudes of the transistor signal are almost independent of the concentration of the mobile buffer. A low concentration of immobile buffer is essential to explain the data. 3), A computed signal, where the diffusion coefficients within the matrix are lowered by a factor of 1/10, is depicted in Fig. 5 *D*. The decay time of the signal is distinctly faster than the transistor record. The slow diffusion in the matrix determines the duration of the transistor signal.

Limit of sensitivity

We can clearly identify signals with an amplitude of 200 μV in the noise of the transistor record. This limit corresponds to a vesicle diameter of ~170 nm, if we assume that the 1.4-mV median of the transistor signals corresponds to a release of dense-core vesicles with a diameter of 340 nm in chromaffin cells (23).

If low-noise transistors (27) were used with the same gate area of 40 μm^2, signals with an amplitude of 50 μV could be identified. Such signals would correspond to a vesicle diameter of 105 nm, typical for dense-core vesicles in synapses (28). A detection of smaller synaptic vesicles could be achieved, if smaller transistors were used, so that a larger fraction of the source-drain current would be affected by a localized pH change. For a vesicle diameter of 50 nm on a gate of 0.5 μm^2 we would expect a signal amplitude around 400 μV at a detection limit of ~300 μV that results from an enhanced 1/*f* noise with the smaller size of the transistor gates (27).

CONCLUSION

The bioelectronic device of a chromaffin cell on a field-effect transistor establishes a chemical cell-semiconductor synapse where the presynaptic release of vesicles is coupled to a postsynaptic response of an electronic current. Field-effect transistors are a novel tool to monitor the exocytosis of vesicles with a time resolution similar to that of amperometry. Because of signaling by protons, through this method it is possible to probe vesicles with electrochemically inactive hormones or transmitters. Large transistor arrays with a pH-sensitive oxide surface as fabricated by extended CMOS technology (29) may allow parallel recordings of many cells to achieve reliable statistics for physiological experiments and drug screening. For neuronal networks on semiconductor chips, we may envisage a simultaneous mapping of the electrical activity and of synaptic transmission.

We thank Jakob Soerensen and Uri Ashery for an introduction to the preparation of chromaffin cells, and Erwin Neher and Moritz Voelker for fruitful comments on a draft of the manuscript.

The project was funded by the European Union (Information Society Technologies program).

REFERENCES

1. Leszczyszyn, D. J., J. A. Jankowski, O. H. Viveros, E. J. Diliberto, J. A. Near, and R. M. Wightman. 1991. Secretion of catecholamines from individual adrenal-medullary chromaffin cells. *J. Neurochem.* 56:1855–1863.
2. Chow, R. H., L. von Rüden, and E. Neher. 1992. Delay in vesicle fusion revealed by electrochemical monitoring of single secretory events in adrenal chromaffin cells. *Nature*. 356:60–63.
3. Dernick, G., L. W. Gong, L. Tabares, G. A. de Toledo, and M. Lindau. 2005. Patch amperometry: high-resolution measurements of single-vesicle fusion and release. *Nat. Methods*. 2:699–708.
4. Haller, M., C. Heinemann, R. H. Chow, R. Heidelberger, and E. Neher. 1998. Comparison of secretory responses as measured by membrane capacitance and by amperometry. *Biophys. J.* 74:2100–2113.
5. Oheim, M., D. Loerke, R. H. Chow, and W. Stühmer. 1999. Evanescent-wave microscopy: a new tool to gain insight into the control of transmitter release. *Phil. Trans. R. Soc. Lond. B*. 354: 307–318.
6. Amatore, C., Y. Bouret, and L. Midrier. 1999. Time-resolved dynamics of the vesicle membrane during individual exocytotic secretion events, as extracted from amperometric monitoring of adrenaline exocytosis from chromaffin cells. *Chem. Eur. J.* 5:2151–2162.
7. Lindau, M., and G. A. de Toledo. 2003. The fusion pore. *Biochim. Biophys. Acta*. 1641:167–173.
8. Fromherz, P. 2002. Electrical interfacing of nerve cells and semiconductor chips. *ChemPhysChem*. 3:276–284.
9. Pothos, E. N., E. Mosharov, K. P. Liu, W. Setlik, M. Haburcak, G. Baldini, M. D. Gershon, H. Tamir, and D. Sulzer. 2002. Stimulation-dependent regulation of the pH, volume and quantal size of bovine and rodent secretory vesicles. *J. Physiol.* 542:453–476.
10. Winkler, H., and E. Westhead. 1980. The molecular organization of adrenal chromaffin granules. *Neuroscience*. 5:1803–1823.
11. Bergveld, P. 1970. Development of an ion-sensitive solid-state device for neurophysiological measurements. *IEEE Trans. Biomed. Eng.* 17:70–71.
12. Glombik, M. M., and H. Gerdes. 2000. Signal-mediated sorting of neuropeptides and prohormones: secretory granule biogenesis revisited. *Biochimie*. 82:315–326.
13. Straub, B., E. Meyer, and P. Fromherz. 2001. Recombinant maxi-K channels on transistor, a prototype of iono-electronic interfacing. *Nat. Biotechnol.* 19:121–124.

14. Brittinger, M., and P. Fromherz. 2005. Field-effect transistor with recombinant potassium channels: fast and slow response by electrical and chemical interactions. *Appl. Phys. A*. 81:439–447.

15. Nagy, G., U. Matti, R. B. Nehring, T. Binz, J. Rettig, E. Neher, and J. B. Sorensen. 2002. Protein kinase C-dependent phosphorylation of synaptosome-associated protein of 25 kDa at Ser(187) potentiates vesicle recruitment. *J. Neurosci.* 22:9278–9286.

16. Jonas, P. 1995. Fast application of agonists to isolated membrane patches. *In* Single-Channel Recording. B. Sakmann and E. Neher, editors. Plenum Press, New York. 231–243.

17. Lambacher, A., and P. Fromherz. 2002. Luminescence of dye molecules on oxidized silicon and fluorescence interference contrast microscopy of biomembranes. *J. Opt. Soc. Am. B*. 19:1435–1453.

18. Mitra, M., and R. Lal. 1992. Study of proton binding-sites at the silicon dioxide-electrolyte interface with conductance spectroscopy. *J. Electrochem. Soc.* 139:1706–1714.

19. Scales, P. J., F. Grieser, T. W. Healy, L. R. White, and D. Y. C. Chan. 1992. Electrokinetics of the silica solution interface – a flat-plate streaming potential study. *Langmuir.* 8:965–974.

20. Press, W. H., S. A. Teukolsky, and W. T. Vetterling. 1993. Numerical Recipes in C. Cambridge University Press, Cambridge.

21. von Rüden, L., A. G. Garcia, and M. G. Lopez. 1993. The Mechanism of Ba^{2+}-induced exocytosis from single chromaffin cells. *FEBS Lett.* 336:48–52.

22. Blackmore, C. G., A. Varro, R. Dimaline, L. Bishop, D. V. Gallacher, and G. J. Dockray. 2001. Measurement of secretory vesicle pH reveals intravesicular alkalinization by vesicular monoamine transporter type 2 resulting in inhibition of prohormone cleavage. *J. Physiol. (Lond.).* 531:605–617.

23. Coupland, R. E. 1968. Determining sizes and distribution of sizes of spherical bodies such as chromaffin granules in tissue sections. *Nature.* 217:384–388.

24. Stevens, C. F. 2003. Neurotransmitter release at central synapses. *Neuron.* 40:381–388.

25. Junge, W., and S. McLaughlin. 1987. The role of fixed and mobile buffers in the kinetics of proton movement. *Biochim. Biophys. Acta.* 890:1–5.

26. Marszalek, P. E., B. Farrell, P. Verdugo, and J. M. Fernandez. 1997. Kinetics of release of serotonin from isolated secretory granules. 2. Ion exchange determines the diffusivity of serotonin. *Biophys. J.* 73: 1169–1183.

27. Voelker, M., and P. Fromherz. 2006. Nyquist noise of cell adhesion detected in a neuron-silicon transistor. *Phys. Rev. Lett.* 96: 228102.

28. Klyachko, V. A., and M. B. Jackson. 2002. Capacitance steps and fusion pores of small and large-dense-core vesicles in nerve terminals. *Nature.* 418:89–92.

29. Lambacher, A., M. Jenkner, M. Merz, B. Eversmann, R. A. Kaul, F. Hofmann, R. Thewes, and P. Fromherz. 2004. Electrical imaging of neuronal activity by multi-transistor-array (MTA) recording at 7.8 μm resolution. *Appl. Phys. A.* 79:1607–1611.